Vision Research 50 (2010) 2439–2444

Contents lists available at ScienceDirect

Vision Research

journal homepage: www.elsevier.com/locate/visres

# Combined effect of wavelength and polarization in double-pass retinal images in the human eye

Juan M. Bueno *, Guillermo M. Pérez

*Laboratorio de Óptica, Centro de Investigación en Óptica y Nanofísica (CiOyN), Universidad de Murcia, Campus de Espinardo, 30100 Murcia, Spain*

ARTICLE INFO

*Article history:*
Received 17 February 2010
Received in revised form 2 September 2010

*Keywords:*
Retinal image quality
Polarization
Mueller matrix
Polarimetry
Diattenuation

ABSTRACT

A polychromatic double-pass setup was developed to study the effects of wavelength and polarization on retinal image quality. The results show that the central part of the images was similar for all wavelengths (543, 633 and 780 nm) and polarization states. However, the image tails increased significantly when using infrared light for all the polarization states used. For the set of subjects involved in the study, ocular diattenuation presented individual differences, however significant changes were not found across the different wavelengths. Moreover the Stokes vectors providing the maximum intensity transmittance varied across subjects and corresponded to elliptically polarized light. These non-negligible diattenuation effects might affect the performance of clinical devices which only take into account ocular birefringence.



## 1. Introduction

There has been an early interest in exploring the properties of the human ocular media, in particular the retinal image quality, as a function of wavelength. Early studies reported that ocular fundus reflectance was higher with infrared than with visible light (Delori & Pflibsen, 1989). Infrared light was also found to provide improved imaging of deeper retinal features than visible light (Elsner, Burns, Weiter, & Delori, 1996). Double pass (DP) retinal images acquired with near-infrared light showed a larger halo of light compared with those obtained with green light (Llorente, Díaz-Santana, Lara-Saucedo, & Marcos, 2003; López-Gil & Artal, 1997).

The polarization properties of the living human eye have extensively been studied (see for instance Bour (1991)). Both corneal and retinal birefringence were reported as the main contributors (klein Brink & van Blokland, 1988; van Blokland & Verhelst, 1987). The changes in the polarization properties are used in clinical environments as an indicator of glaucoma (Dreher, Reiter, & Weinreb, 1992; Zhou & Weinreb, 2002). Since different wavelengths penetrate into the retina differentially, as light penetrates deeper there is an increase in scattering and therefore in ocular depolarization (Baumann, Goetzinger, Pircher, & Hitzenberger, 2009; Bueno, 2001; van Blokland & van Norren, 1986). Diattenuation ($D$) might also be present in the human eye to a lesser extent (Bueno & Artal, 2008; Twietmeyer, Chipman, Elsner, Zhao, & VanNasdale, 2008).

Since wavelength and polarization might have influence on the retinal image (Bueno & Artal, 2001; Gorrand, Alfieri, & Boire, 1984), the combination of these two factors should potentially affect the performance of devices based on collecting light scattered back in the retina. However, studies about the dependence between ocular reflectance and the polarization state of the incident light (i.e. diattenuation (Chipman, 1995)) are scarce in the literature.

In this sense, the present study explores the interactions between polarization and wavelength and how these affect the retinal image quality. We modified a DP apparatus to record retinal images with three different wavelengths, while changing the polarization state of the incident light. By further analyzing the DP images, ocular $D$ as a function of wavelength was also quantified. Since DP images provide information on the whole eye, the values of $D$ here reported correspond to the contribution of the central cornea and the fovea.

## 2. Methods

### 2.1. Apparatus and experimental procedure

A schematic diagram of the experimental system used in this work is depicted in Fig. 1. This is a polychromatic DP ophthalmoscopic system, which incorporates a polarization states generator (PSG) in the first passage. It operates at three different wavelengths: green (543 nm) coming from a He–Ne laser, and red (633 nm) and near-infrared (780 nm) provided by two diode lasers. Two removable mirrors (RM1 and RM2) permit the selection of the desired wavelength.

The apparatus is a modified version of that described in (Bueno, Berrio, Ozolinsh, & Artal, 2004). Each collimated laser beam passes

* Corresponding author.
*E-mail address:* bueno@um.es (J.M. Bueno).

0042-6989/$ - see front matter © 2010 Published by Elsevier Ltd.
doi:10.1016/j.visres.2010.09.005

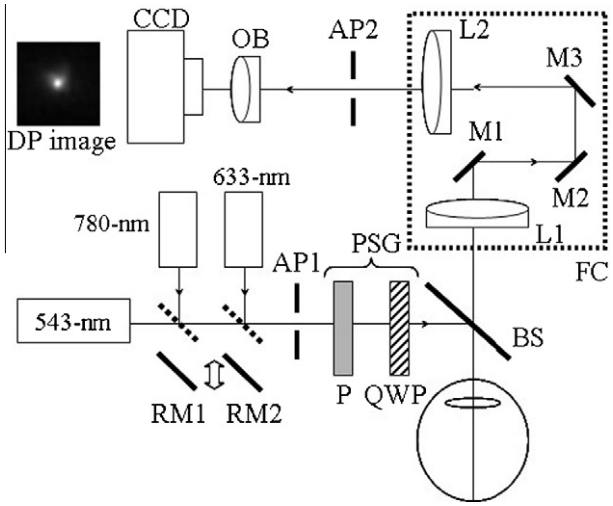


**Fig. 1.** Schematic diagram of the polychromatic DP ophthalmoscopic system including a generator of polarization states in the ingoing pathway: P, linear polarizer, QWP, rotary quarter-wave plate, BS, beam splitter, L1 and L2, achromatic doublets; AP1 and AP2, artificial pupils; RM1 and RM2, removable mirrors; M1–M3, mirrors; FC, focus corrector; OB, objective.

the PSG and enters the eye. The PSG consists of a fixed vertical linear polarizer (P) and a rotatory quarter-wave plate (QWP). In the second passage, the light emerging the eye passes by an optometer-based focus corrector system (FC) and reaches a CCD camera (DP image). FC is composed of two achromatic doublets (L1 and L2) separated by three mirrors, two of them (M2 and M3) placed on a moving stage in order to correct for the spherical refractive error of the eye for each wavelength. Artificial pupils AP1 and AP2 are conjugated with the eye's pupil to control the size of the beam in the incoming and outgoing pathways (1.5 and 5 mm in diameter respectively).

Measurements were carried out in five normal healthy and well-trained adult subjects (mean age: 31.8 ± 2.4 years). All presented a best corrected visual acuity 20/20 or higher. For each subject, all images were acquired in a single experimental session. During recording, head's movements were minimized by using a bite-bar mounted on a three-axis positioning stage. Each eye's pupil was dilated and accommodation was paralyzed with two drops of tropicamide (1%). Before recording the DP images and for each experimental condition, the operator looked for the best focus by moving FC, while the subject directly stared at the conveniently attenuated point source.

Four independent polarization states were produced in the PSG by placing the fast axis of the QWP at four different angles (see Bueno et al. (2004) for further information). Sets of four DP retinal images (1 − *s* exposure, 2.5° of visual field) were recorded for each orientation ($I_1^{(j)}$, $I_2^{(j)}$, $I_3^{(j)}$, $I_4^{(j)}$; *j* = 1–4). The experimental setup itself was firstly calibrated as explained elsewhere (Bueno, 2000) to ensure independent incoming polarization states and, hence, the contribution of the residual polarization properties of the optical elements (in particular *D*) was compensated.

A background image (taken from an empty field) was subtracted from every DP raw image $I_i^{(j)}$ (*i*, *j* = 1–4). Then, each set of polarimetric DP images was averaged to compute the final DP image. The resulting images were named as $I_C$, $I_V$, $I_{E1}$, and $I_{E2}$. C, V, E1 and E2 represent right-circular, linear vertical, and two elliptical polarization states respectively. Two parameters were computed from these final DP images: the averaged intensity radial profile (López-Gil & Artal, 1997; Santamaría, Artal, & Bescós, 1987) and a parameter of scattering (POS) defined as (Westheimer & Liang, 1995):

$$\mathrm{POS} = \mathrm{Int}(20:60)/\mathrm{Int}(0:20) \quad (1)$$

where Int(20:60) and Int(0:20) are the areas under the normalized intensity profile between 20 and 60 arcmin, and between 0 and 20 arcmin respectively. All calculations were done in MATLAB (The MathWorks, Inc., Natick, MA).

For the second part of the experiment DP images $I_C$, $I_V$, $I_{E1}$, and $I_{E2}$ were used to compute the spatially resolved elements of the first row of the Mueller matrix: $M_{00}$, $M_{01}$, $M_{02}$, and $M_{03}$ (Bueno, Hunter, Cookson, Kisilak, & Campbell, 2007). From these spatially resolved elements, the averaged intensity values were calculated in a squared central area (8 × 8 arcmin). This region was the core of the images (combining the effects of both central cornea and fovea). The parameter *D* (which ranges between 0 and 1) was computed as (Chipman, 1995):

$$D = \frac{\sqrt{M_{01}^2 + M_{02}^2 + M_{03}^2}}{M_{00}} \quad (2)$$

Moreover, the polarization state associated with the maximum intensity transmittance (diattenuation axis) is expressed as (Barakat, 1987):

$$S_{\max} = \begin{pmatrix} 1 \\ \cos(2\varphi)\cdot\cos(2\chi) \\ \cos(2\varphi)\cdot\sin(2\chi) \\ \sin(2\varphi) \end{pmatrix} = \begin{pmatrix} 1 \\ M_{01}/M_{SQ} \\ M_{02}/M_{SQ} \\ M_{03}/M_{SQ} \end{pmatrix} \quad \text{with}$$
$$M_{SQ} = \sqrt{M_{01}^2 + M_{02}^2 + M_{03}^2} \quad (3)$$

where $2\varphi$ and $2\chi$ are the coordinates of the polarization states on the Poincaré sphere (i.e. $\varphi$ and $\chi$ are respectively the ellipticity and the azimuth).

## 3. Results

### 3.1. Polarization, wavelength and double-pass retinal image quality estimates

Fig. 2a depicts the normalized averaged intensity radial profile for linearly polarized light (image $I_V$) and the three wavelengths. Each line is the mean for all subjects. The central part of the radial profiles is similar for the three wavelengths, but when going towards the periphery, the amount of infrared light is larger as shown in the inset. Fig. 2b shows the total intensity at the central area of the DP image (~3 arcmin), averaged values for all the subjects as a function of the incoming polarization states. Across the wavelengths, no significant differences were found among the different polarization states (student paired *t*-test). Across polarization states, infrared light was statistically different from green light ($p = 0.02$).

Fig. 3a plots the POS averaged for all subjects, for the four polarization states and the three wavelengths. For all polarization states the POS was higher for infrared light. Across polarization states, the largest difference also corresponded to infrared light. This is better observed in Fig. 3b, which represents the mean across the four polarization states, and all subjects, as a function of wavelength. According to student's paired *t*-test, across all polarization states, POS for infrared light significant differed from those POS values for green and red light ($p < 0.05$). Across all wavelengths, states E1 and E2 were significantly different from V ($p = 0.02$ and $p = 0.04$ respectively) but not from C.

### 3.2. Wavelength and ocular diattenuation

As an example, Fig. 4 depicts the normalized central intensity of the DP images $I_C$, $I_V$, $I_{E1}$, and $I_{E2}$ for a particular subject. Since the

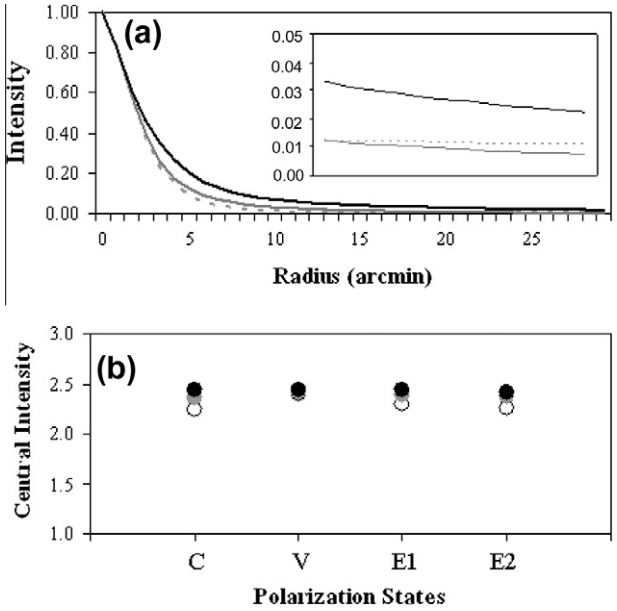


**Fig. 2.** (a) Normalized intensity radial profiles of the DP images acquired with linear polarized light for green (grey dashed line), red (grey solid line) and infrared (black line). Each line is the mean for all subjects. The inset shows the profiles between 20 and 30 arcmin. (b) Total intensity at the central area of the DP image averaged for all subjects as a function of the polarization states in the PSG for green (white), red (grey) and infrared (black) light.

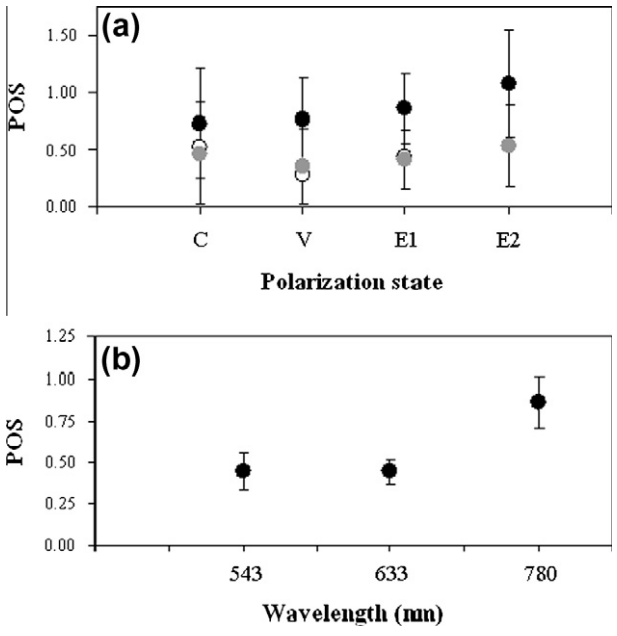


**Fig. 3.** (a) POS values averaged for all subjects as a function of the polarization state in PSG for the three wavelengths. Symbols are the same as in the previous figure. (c) POS values averaged for all subjects and polarization states as a function of wavelength.

maximum intensity value of the DP images for each subject depends on the polarization state of the incident light, the intensity values for each wavelength were normalized to the maximum for a better comparison. The difference between the maximum and the minimum intensity depended on both the subject and the wavelength. By considering all subjects, polarization states and wavelengths, only E1 for infrared light was found to be significantly different from E1 for green ($p = 0.02$) and red light ($p = 0.03$).

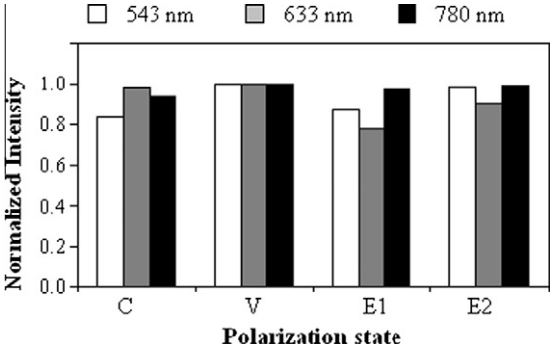


**Fig. 4.** Normalized intensity for the central part of DP images in one subject as a function of the polarization state for every wavelength.

Fig. 5 shows the spatially resolved $M_{0j}$ ($j = 0$–3) elements computed as explained in the Section 2 for the three wavelengths in the same subject as in Fig. 4.

From these elements, the values of $D$ were calculated as indicated above. Fig. 6 depicts the values of $D$ for the subject in Fig. 5 (white bars), together with the averaged value across all subjects for the three wavelengths (grey bars). For this particular set of eyes, the value of $D$ ranges between 0.05 and 0.17 for green light, from 0.07 to 0.15 for red light, and between 0.04 and 0.16 for infrared light. We also include the value of $D$ (for a wavelength of 633 nm) from (Bueno & Artal, 2008). Results show that differences in $D$ across wavelengths are non significant, at least within the accuracy of the technique that we used here.

Finally, using Eq. (3) we computed the "optimum Stokes vector" which provides the maximum transmittance (i.e. the diattenuation axis) for every subject and wavelength. The corresponding values of ellipticity and azimuth are shown in Fig. 7. We decided to represent $2\varphi$ and $2\chi$, since these are the coordinates of the polarization states on the Poincaré sphere (latitude and longitude respectively).

## 4. Discussion

### 4.1. Double-pass retinal image quality, wavelength and polarization

The polychromatic DP ophthalmoscope designed in this work was used to evaluate the combined effect of polarization and wavelength on retinal image quality. Previous studies reported the DP system as a reliable tool for retinal image quality estimates in both visible and infrared light (Díaz-Doutón et al., 2006; López-Gil & Artal, 1997).

It has already been reported that infrared retinal images show a broader tail light (López-Gil & Artal, 1997; Westheimer & Campbell, 1962), which is associated with deeper penetration of infrared light into the choroid, and with an increase of both intraocular scattering and depolarization. Conversely, green light does not penetrate so effectively and hence, the scattering effects are lower.

Most previous works were carried out with linearly polarized light. Our results agree well with those previous reports, but we also include the effects of circular and elliptical polarized light. We found that the central part of the DP images were similar for all polarization states and wavelengths (Fig. 2). Maximum differences among all polarization states and wavelengths were about 6 %.

Since the central part of the DP images contains information on the ocular aberrations, the low variability on this region agrees well with the fact that ocular aberrations (or alternatively, the retinal image quality) hardly depend on the polarization state of the incident light (Bueno & Artal, 2001; Bueno, Berrio, & Artal, 2003; Marcos, Díaz-Santana, Llorente, & Dainty, 2002; Prieto, Vargas-Martín, McLellan, & Burns, 2002). However, combinations of

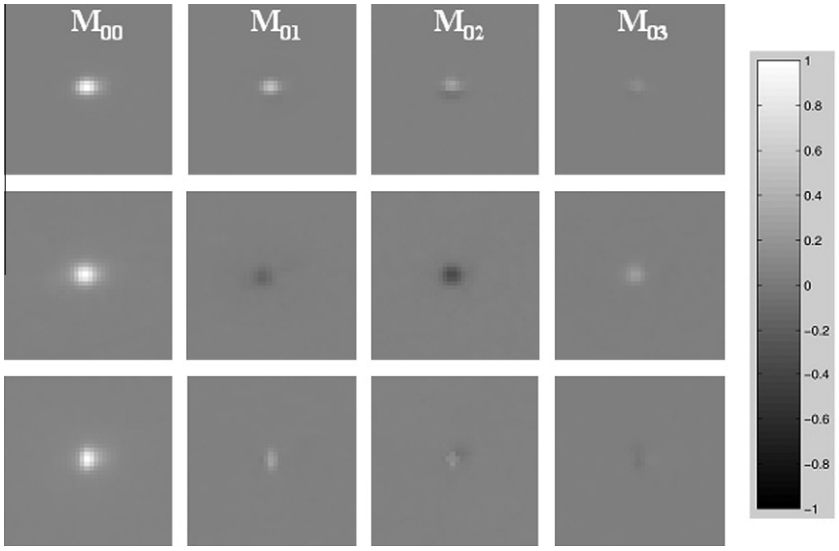


**Fig. 5.** Example of spatially resolved elements of the first row of the Mueller matrix in one of the subjects involved in the study for three different wavelengths (upper panels, green; medium panels, red; bottom panels, infrared). The grey level code is shown at the right and images subtend 31.2 arcmin.

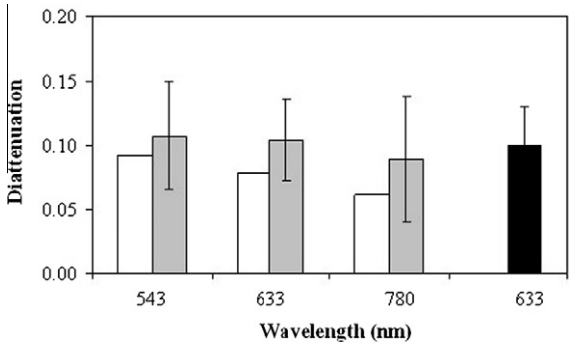


**Fig. 6.** Diattenuation values for each wavelength for the subject of Fig. 5 (white bars) and the averaged values across all subjects (grey bars). As a comparison the result for red light in (Bueno and Artal, 2008) has also been included (black bar). Error bars indicate the standard deviation.

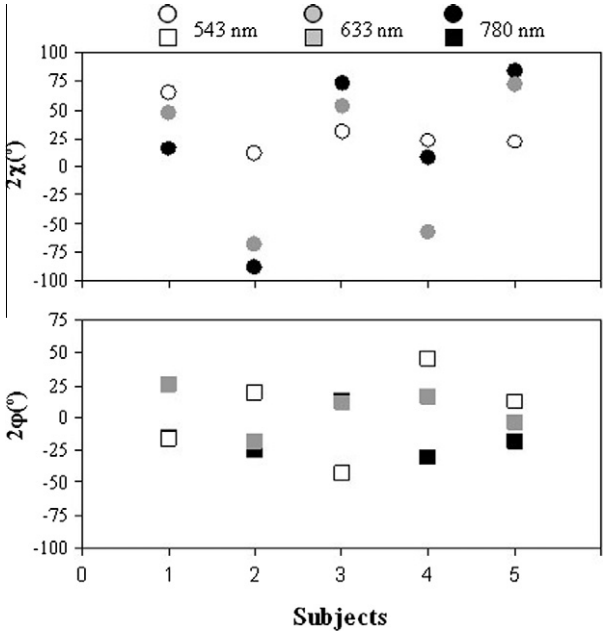


**Fig. 7.** Coordinates on the Poincaré sphere of the Stokes vectors ($S_{max}$) providing maximum intensity transmittance at the central part of double-pass images for all subjects and wavelengths.

in-and-out polarization states might significantly underestimate the retinal image quality, as early reported by Röhler, Miller and Aberl (1969) and later confirmed by others (Bueno & Artal, 2001; Williams, Brainard, McMahon, & Navarro, 1994).

Since the core of the DP image is related to the light guided through the photoreceptors, results here presented indicate a major retinal layer as the responsible for the retinal reflection for light within the range 532–780 nm. This is in good agreement with the work by Elsner and colleagues (Elsner et al., 1996), who found that the fraction of fundus reflectance containing the guided component was independent of wavelength across the range from 550 to 750 nm. Moreover, this also agrees with other studies reporting that the reflection of both polarized and non-polarized components occurs at a single layer (van Blokland & van Norren, 1986) and that different configurations of linear polarizations hardly affect the best focus position (Bueno, 2001).

Although the central portion of the DP images remained similar, the increase in the scattering halo of the infrared DP images leads to a reduction in the retinal image quality. Along this work, we have showed that this increase occurs for all polarization states (Fig. 3). Moreover, we found that DP images for red light do not differ significantly from those corresponding to green light.

Despite the worsening of retinal image quality with infrared light, the ocular wavefront aberrations (beyond defocus) computed using different aberrometers have been reported to be nearly constant across a wide wavelength range (Fernández & Artal, 2008; Fernández et al., 2005; Llorente et al., 2003). This could be expected since unlike the DP method, aberrometers do not have the scattering effects into account and the retinal image quality might be overestimated (Díaz-Doutón et al., 2006).

We conclude that, despite the complicated ocular polarization properties, the retinal image quality is nearly independent on the polarization states of the incident light for each wavelength. Additionally, for every individual polarization state, this image quality is always worse for infrared light than for green and red. That is, for a given wavelength from green to near-infrared, a major improvement in the ocular optics could not be achieved by modifying the polarization state of the incoming light beam, which agrees

with the fact that the human eye is not sensitive to different polarization states (Bour, 1991).

The present results might also suggest that techniques which are based on collecting the light scattered back in the retina would not be significantly affected by the polarization state of the illumination channel. However, it has recently been demonstrated that extended fundus images can be improved by varying the incident polarization state or using depolarized light (Bueno et al., 2007; Burns, Elsner, Mellem-Kairala, & Simmons, 2003; Song, Zhao, Chui, Qi, & Burns, 2008). The reasons for this are the non-null and spatially changing $D$ values of the human eye (Bueno & Artal, 2008; Twietmeyer et al., 2008) as extensively discussed in the next section.

### 4.2. Ocular diattenuation

An optical system (in particular the eye) shows properties of $D$ when there is a non-null dependence between the transmitted/reflected intensity and the polarization state of the incoming light. Since this parameter ranges between 0 and 1, the closer the value to 1, the higher the dependence between the incident polarization state and the intensity of the light reflected at the retinal fundus (and emerging from the eye).

For the subjects involved in this study, the central part of the elements $M_{0j}$ ($j = 0$–3) of the Mueller matrix were different from zero. All elements but $M_{00}$ might have either positive or negative values. These elements were particular, not only for every subject but also for each wavelength (see Fig. 5). As a result, the parameter $D$ has non-null values (Fig. 6), indicating some dependence between the ocular intensity transmittance and the polarization state of the incident light.

Despite the number of subjects is small, the results give an insight into the values of ocular $D$ in normal eyes. For a more general conclusion, additional experiments involving more subjects would be required. Looking into individual results, we found that the ranges of $D$ across the subjects were similar for the three wavelengths used in this study. For every subject, differences across wavelengths ranged between 0.01 and 0.06. In particular, the averaged $D$ values were 0.11, 0.10 and 0.09 for green, red and infrared light respectively. This result indicates that, within the accuracy of our measurements and our small set of subjects, there is a slight dependence between the polarization state of the incident light and the intensity transmitted by the eye, and this dependence is similar for the three wavelengths.

Studies on ocular birefringence and $D$ in the living human eye are scarce in the literature. Most studies exploring the polarization sensitivity of the eye were based on measurements of dichroism (see Bueno and Artal (2008) and Chipman (1995) for more information on this parameter) and they hardly used polarimetric techniques.

Using Mueller-matrix polarimetry (633 nm wavelength), the $D$ values for an area around the post-mortem human optic nerve head ranged between 0 and 0.11 (Dreher et al., 1992). Later some measurements (with light of 785 nm) reported values of ~0.03 for the macula area and ~0.06 for the optic nerve head in living human eyes (Pelz, 1997). Significant differences between normal and glaucomatous eyes (at the retinal nerve fiber layer for light of 632.8 nm) were found: values between 0.05 and 0.19 for the former and between 0.01 and 0.08 for the latter (Naoun, Louis-Dorr, Allé, Sablon, & Benoit, 2005). More recently, Twietmeyer and co-workers (2008) modified a clinical polarimeter that uses a 780 nm laser source to explore polarization properties at the optic nerve head and at the macular area. The values of $D$ ranged between 0.07 and 0.11 (mean: 0.09 ± 0.05) for normal eyes, and between 0.07 and 0.10 (mean: 0.08 ± 0.05) for glaucomatous eyes.

Here, the results of ocular $D$ agree with those found in the literature. Despite the technique used in Bueno and Artal (2008) was slightly different from the one here used, the averaged $D$ value for a wavelength of 633 nm was similar (0.10 ± 0.03). The averaged $D$ value for red light in this work has been 0.10 ± 0.04.

The main drawback of our technique is that the individual contribution of the different ocular structures (cornea, lens and retina) can not be separated. However, since low $D$ values were reported for *in vitro* corneas and lenses (see Bueno and Artal (2008) and references therein), it could be assumed that $D$ values here reported would be produced by the retina. Moreover, it has also been showed that the axes of ocular birefringence and $D$ differ (Bueno & Artal, 2008), what indicates that the main source of $D$ in the healthy human eye is the retina (probably the Henle fiber layer).

Since the values of $D$ are different from zero, an incoming polarization state providing a maximum in the transmitted intensity is expected. In spite of the size of our sample, the results show that these optimum Stokes vectors vary with both, the subject and the wavelength (Fig. 7). Although most of these optimum Stokes vectors correspond to elliptically polarized light, the vectors for green light are, on average, closer to the equatorial plane (i.e. linearly polarized light, mean ~5°) that those associated with red and infrared light (19° and −20° respectively). Moreover, the values of azimuth and ellipticity for red and infrared light seem to be closer to each other (average difference ~12°).

As above discussed, this weak (but no null) dependence between the light reflected at the retina, as well as the different polarization-dependence of the structures located across the retinal fundus, are the basis for retinal fundus image improvement reported by different authors (Bueno et al., 2007; Burns, Elsner, Mellem-Kairala, & Simmons, 2003; Mellem-Kairala, Elsner, Weber, Simmons, & Burns, 2005; Miura et al., 2005; Song et al., 2008; Weber, Cheney, Smithwick, & Elsner, 2004). These results might have an impact on glaucoma imaging techniques too, since the Mueller matrix is not calculated in clinical devices and only the effects of ocular birefringence are taken into account. Since depolarization and $D$ affect the measured ocular retardation (Bueno, 2002, 2004), both over- and underestimation might lead to an erroneous diagnosis of certain pathologies (glaucoma in particular). In this sense, an in-depth study on the spatial distribution of $D$ across the retina (mainly macular region and optic nerve head) in healthy and pathological eyes will be of particular interest.

## Acknowledgments

The research has been supported by the Ministerio de Educación y Ciencia, Spain (Grant FIS2007-64765). Authors thank P. Artal for valuable discussions during the early stages of this work.

## References

Barakat, R. (1987). Conditions for the physical realizability of polarization matrices characterizing passive systems. *Journal of Modern Optics, 34*, 1535–1544.

Baumann, B., Goetzinger, E., Pircher, M., & Hitzenberger, C. (2009). Measurements of depolarization distribution in the healthy human macula by polarization sensitive OCT. *Journal of Biophotonics, 2*, 426–434.

Bour, L. J. (1991). Polarized light and the eye. In W. N. Charman (Ed.). *Vision Optics and Instrumentation* (vol. 1, pp. 310–325). New York: Macmillan Press.

Bueno, J. M. (2000). Measurement of parameters of polarization in the living human eye using imaging polarimetry. *Vision Research, 40*, 3791–3799.

Bueno, J. M. (2001). Depolarization effects in the human eye. *Vision Research, 41*, 2687–2696.

Bueno, J. M. (2002). Polarimetry in the human eye using an imaging linear polariscope. *Journal of Optics A: Pure and Applied Optics, 4*, 553–561.

Bueno, J. M. (2004). The influence of depolarization and corneal birefringence on ocular polarization. *Journal of Optics A: Pure and Applied Optics, 6*, S91–S99.

Bueno, J. M., & Artal, P. (2001). Polarization and retinal image quality estimates in the human eye. *Journal of the Optical Society of America A, 18*, 489–496.

Bueno, J. M., & Artal, P. (2008). Average double-pass ocular diattenuation using foveal fixation. *Journal of Modern Optics, 55*, 849–859.
Bueno, J. M., Berrio, E., & Artal, P. (2003). Aberro-polariscope for the human eye. *Optics Letters, 28*, 1209–1211.
Bueno, J. M., Berrio, E., Ozolinsh, M., & Artal, P. (2004). Degree of polarization as an objective method of estimating scattering. *Journal of the Optical Society of America A, 21*, 1316–1321.
Bueno, J. M., Hunter, J. J., Cookson, C. J., Kisilak, M. L., & Campbell, M. C. W. (2007). Improved scanning laser fundus imaging using polarimetry. *Journal of the Optical Society of America A, 24*, 1337–1348.
Burns, S. A., Elsner, A. E., Mellem-Kairala, M. B., & Simmons, R. B. (2003). Improved contrast of subretinal structures using polarization analysis. *Investigative Ophthalmology and Visual Science, 44*, 4061–4068.
Chipman, R. A. (1995). Polarimetry. In M. Bass (Ed.), *Handbook of optics* (vol. 2, 2nd ed., pp. 22.1–22.37). New York: McGraw-Hill.
Delori, F. C., & Pflibsen, K. P. (1989). Spectral reflectance of the human ocular fundus. *Applied Optics, 28*, 1061–1077.
Díaz-Doutón, F., Benito, A., Pujol, J., Arjona, M., Güell, J. L., & Artal, P. (2006). Comparison of the retinal image quality with a Hartmann–Shack wavefront sensor and a double-pass instrument. *Investigative Ophthalmology and Visual Science, 47*, 1710–1716.
Dreher, A. W., Reiter, K., & Weinreb, R. N. (1992). Spatially resolved birefringence of the retinal never fiber layer assessed with a retinal laser ellipsometer. *Applied Optics, 31*, 3730–3735.
Elsner, A. E., Burns, S. A., Weiter, J. J., & Delori, F. C. (1996). Infra-red imaging of subretinal structures. *Vision Research, 36*, 191–205.
Fernández, E. J., & Artal, P. (2008). Ocular aberrations up to the infrared range: From 632.8 to 1070 nm. *Optics Express, 16*, 21199–21208.
Fernández, E. J., Unterhuber, A., Prieto, P. M., Hermann, B., Drexler, W., & Artal, P. (2005). Ocular aberrations as a function of wavelength in the near infrared measured with a femtosecond laser. *Optics Express, 13*, 400–409.
Gorrand, J. M., Alfieri, R., & Boire, J. Y. (1984). Diffusion of the retinal layers of the living human eye. *Vision Research, 24*, 1097–1106.
klein Brink, S. C., & van Blokland, G. J. (1988). Birefringence of the human fovea area assessed in vivo with Mueller-matrix ellipsometry. *Journal of the Optical Society of America A, 5*, 49–57.
Llorente, L., Díaz-Santana, L., Lara-Saucedo, D., & Marcos, S. (2003). Aberrations of the human eye in visible and near infrared illumination. *Optometry and Vision Science, 80*, 26–35.
López-Gil, N., & Artal, P. (1997). Comparison of double pass estimates of the retinal image quality obtained with green and near infrared light. *Journal of the Optical Society of America A, 14*, 961–971.
Marcos, S., Díaz-Santana, L., Llorente, L., & Dainty, J. C. (2002). Ocular aberrations with laser ray tracing and Shack–Hartmann: Does polarization play a role? *Journal of the Optical Society of America A, 19*, 1063–1072.
Mellem-Kairala, M. B., Elsner, A. E., Weber, A., Simmons, R. B., & Burns, S. A. (2005). Improved contrast of peripapillary hyperpigmentation using polarization analysis. *Investigative Ophthalmology and Visual Science, 46*, 1099–1106.
Miura, M., Elsner, A. E., Weber, A., Cheney, M. C., Oshako, M., Usui, M., et al. (2005). Imaging polarimetry in central serous chorioretinopathy. *American Journal of Ophthalmology, 140*, 1014–1019.
Naoun, O. K., Louis-Dorr, V., Allé, P., Sablon, J. C., & Benoit, A. M. (2005). Exploration of the retinal nerver fiber layer thickness by measurement of the linear dichroism. *Applied Optics, 44*, 7074–7082.
Pelz, B. C. E. (1997) Entwicklung eines elektrooptischen Ellipsometers zur in vivo Evaluation der retinalen Nervenfaserschicht und der Hornhaut des menschlichen Auges. PhD thesis, Universität Heidelberg.
Prieto, P. M., Vargas-Martín, F., McLellan, J. S., & Burns, S. A. (2002). The effect of polarization on ocular wave aberration measurements. *Journal of the Optical Society of America A, 19*, 809–814.
Röhler, R., Miller, U., & Aberl, M. (1969). Zur Messung der Modulations-Ubertragungsfunktion des lebenden mensclichen Auges im reflektierten Licht. *Vision Research, 9*, 407–427.
Santamaría, J., Artal, P., & Bescós, J. (1987). Determination of the point-spread function of the human eye using a hybrid optical–digital method. *Journal of the Optical Society of America A, 4*, 1109–1114.
Song, H., Zhao, Y., Chui, Y., Qi, X., & Burns, S. A. (2008). Stokes vector analysis of adaptive optics images of the retina. *Optics Letters, 33*, 137–140.
Twietmeyer, K. M., Chipman, R. A., Elsner, A. E., Zhao, Y., & VanNasdale, D. (2008). Mueller matrix retinal imager with optimized polarization conditions. *Optics Express, 16*, 21339–21354.
van Blokland, G. J., & van Norren, D. (1986). Intensity and polarization of light scattered at small angles from the human fovea. *Vision Research, 26*, 485–494.
van Blokland, G. J., & Verhelst, S. C. (1987). Corneal polarization in the living human eye explained with a biaxial model. *Journal of the Optical Society of America A, 4*, 82–90.
Weber, A., Cheney, M. C., Smithwick, Q. Y. J., & Elsner, A. E. (2004). Polarimetric imaging and blood vessel quantification. *Optics Express, 12*, 5178–5190.
Westheimer, G., & Campbell, F. W. (1962). Light distribution in the image formed by the living human eye. *Journal of the Optical Society of America, 52*, 1040–1044.
Westheimer, G., & Liang, J. (1995). Influence of ocular light scatter on the eye's optical performance. *Journal of the Optical Society of America, 12*, 1417–1424.
Williams, D. R., Brainard, D. H., McMahon, M. J., & Navarro, R. (1994). Double-pass and interferometric measures of the optical quality of the eye. *Journal of the Optical Society of America A, 11*, 3123–3134.
Zhou, Q., & Weinreb, R. N. (2002). Individualized compensation of anterior segment birefringence during scanning laser polarimetry. *Investigative Ophthalmology and Visual Science, 43*, 2221–2228.